MyD88 signaling in nonhematopoietic cells protects mice against induced colitis by regulating specific EGF receptor ligands

Katharina Brandl[a,1], Lei Sun[a,1], Christina Neppl[a,b], Owen M. Siggs[a], Sylvain M. Le Gall[c], Wataru Tomisato[a], Xiaohong Li[a], Xin Du[a], Daniela N. Maennel[b], Carl P. Blobel[c], and Bruce Beutler[a,2]

[a]Department of Genetics, The Scripps Research Institute, La Jolla, CA 92037; [b]Department of Immunology, University of Regensburg, 93042 Regensburg, Germany; and [c]Arthritis and Tissue Degeneration Program, Hospital for Special Surgery, New York, NY 10021

Toll-like receptors (TLRs) trigger intestinal inflammation when the epithelial barrier is breached by physical trauma or pathogenic microbes. Although it has been shown that TLR-mediated signals are ultimately protective in models of acute intestinal inflammation [such as dextran sulfate sodium (DSS)-induced colitis], it is less clear which cells mediate protection. Here we demonstrate that TLR signaling in the nonhematopoietic compartment confers protection in acute DSS-induced colitis. Epithelial cells of MyD88/Trif-deficient mice express diminished levels of the epidermal growth factor receptor (EGFR) ligands amphiregulin (AREG) and epiregulin (EREG), and systemic lipopolysaccharide administration induces their expression in the colon. N-ethyl-N-nitrosourea (ENU)-induced mutations in Adam17 (which is required for AREG and EREG processing) and in Egfr both produce a strong DSS colitis phenotype, and the Adam17 mutation exerts its deleterious effect in the nonhematopoietic compartment. The effect of abrogation of TLR signaling is mitigated by systemic administration of AREG. A TLR→MyD88→AREG/EREG→EGFR signaling pathway is represented in nonhematopoietic cells of the intestinal tract, responds to microbial stimuli once barriers are breached, and mediates protection against DSS-induced colitis.

epidermal growth factor receptor signaling | inflammatory bowel disease | Toll-like receptor signaling | ENU mutagenesis | intestinal homeostasis

Ulcerative colitis and Crohn's disease are chronic inflammatory disorders of the gastrointestinal tract that have been empirically defined by clinical, pathological, endoscopic, and radiological features (1). The onset of inflammatory bowel disease (IBD) typically occurs in the second and third decades of life, and a majority of affected individuals progress to relapsing and chronic disease (2). IBD depends upon host immunity, and both innate and adaptive immune systems have been implicated (3, 4). Evidence from animal models indicates that failure to suppress immunity to the abundant intestinal foreign antigen load can cause inflammation. Maintaining the normal balance between competence to respond to intestinal pathogens and not generating an inflammatory response to commensals appears to depend on the integrity of the mucosal and epithelial barriers (5–7) and regulation of innate and adaptive immune responses in the intestine and draining lymphoid organs (8), insofar as immune activation often leads to induction of proinflammatory signaling pathways (especially via NF-κB) (9). Barrier disruption and immune dysregulation have been shown to result in intestinal inflammation (2, 4) and are implicated in human IBD, although fundamental knowledge of underlying pathogenesis remains poorly understood. Even the most well-established causative mutations, in Nod2 are responsible for only a small fraction of ileal Crohn's disease occurring in white patients (2, 4, 10).

IBD is dependent upon microbial flora within the gut, because in a variety of mouse strains in which spontaneous chronic colitis occurs, disease is not manifested in a germfree state but rapidly emerges when the animals are conventionalized with normal luminal flora or components thereof (4, 11).

Using random germ-line mutagenesis in a sensitized screen, we have attempted to determine which genes normally prevent IBD in mice. Our work disclosed that Velvet (12), a dominant inhibitory allele of the epidermal growth factor receptor (EGFR)-encoding gene Egfr, and wavedX, a viable recessive allele of Adam17, both yield a severe phenotype in this screen. The Velvet phenotype confirms the results of previous studies on Waved-2 mutant mice showing that a defective EGFR causes hypersensitivity to dextran sulfate sodium (DSS) (13–15). EGFR can be activated by several ligands, including epidermal growth factor (EGF), transforming growth factor (TGF)-α, heparin-binding EGF (HBEGF), betacellulin (Btc), amphiregulin (AREG), and epiregulin (EREG). Although mice lacking TGF-α, EGF, or AREG individually do not show any gastrointestinal phenotype, triple null mice lacking EGF, AREG, and TGF-α show duodenal lesions and aberrant ileum architecture (16). Moreover, mice lacking TGF-α or EREG or EGFR kinase-defective Waved-2 mice are highly susceptible to chemically induced colitis using DSS (14, 15, 17).

The protease a disintegrin and metalloprotease (ADAM) 17 processes numerous growth factor precursors, including ligands of the EGF family, by cleaving and releasing them from the cell membrane in a mature, active form. ADAM17-deficient mice are not viable, but a mouse with reduced ADAM17 levels has recently been generated using the exon-induced translational stop strategy and showed increased sensitivity to DSS (13).

Although these studies show the importance of EGFR signaling in intestinal homeostasis, it is not yet clear how EGF ligands are induced in vivo and which EGF ligands are essential for protection. In addition, the cell type in which EGFR signaling occurs to prevent experimental colitis needs to be identified. Some evidence from in vitro studies using colonic epithelial cell lines suggested the possibility that Toll-like receptor (TLR) signaling might induce expression of EGFR ligands (18–21). Also, studies using a model of colitis-associated cancer demonstrate that TLR4-dependent tumorigenesis is associated with activation of EGFR signaling (18). TLRs recognize commensal luminal bacteria and are crucial for colonic epithelial cell regeneration upon DSS-induced injury (5–7). Here we identify TLR→MyD88 signaling in radioresistant cells, presumably epithelial cells, as an essential conduit for induction of EGF ligands, which avert IBD-like disease after DSS challenge. The EGFR ligands AREG and EREG are underexpressed in the epithelial cells of MyD88/Trif double-deficient mice, and are strongly induced by systemic administration of lipopolysaccharide (LPS) in normal mice. Moreover, ENU-induced mutations that disrupt EGFR signaling

IMMUNOLOGY

develop severe colitis when challenged with DSS. MyD88 signaling, which generates EGFR ligands, and EGFR signaling must occur in cells of the nonhematopoietic compartment to avert colitis.

Results

Failure of TLR Signaling in Nonhematopoietic Cells Accounts for the Colitis Phenotype in MyD88/Trif Double-Deficient Mice.

To determine whether TLR-mediated signaling plays an important role in the hematopoietic or in the nonhematopoietic compartment, bone marrow (BM) chimeras were generated in which the donors and/or the recipients were either wild-type (WT) (CD45.1) or double-deficient in the TLR adaptor proteins MyD88 and Trif (CD45.2). Weight loss was monitored daily in individual chimeric mice receiving 2% DSS in drinking water over a period of 7 d. Chimeric mice lacking TLR signaling in hematopoietic cells showed weight loss similar to that observed in WT mice reconstituted with WT BM, demonstrating that TLR-mediated signaling in hematopoietic cells has no significant effect on the course of DSS-induced colitis. In contrast, transplant recipients lacking epithelial TLR signaling showed severe weight loss, regardless of whether the BM donor was WT or MyD88/Trif double-deficient (Fig. 1A). These findings indicate that TLR signaling confers protection when it occurs in radio-resistant cells (presumably cells of the intestinal epithelium). In addition, hematoxylin/eosin (H&E) staining of histologic sections taken from the colons of different chimeric mice demonstrated ulceration, dramatic leukocyte infiltrations, and a complete loss of epithelial architecture in chimeric mice lacking TLR signaling in nonhematopoietic cells (Fig. 1B).

Previous studies showed an important role for MyD88 signaling in hematopoietic cells in DSS colitis (11). We sought to determine whether the difference between the present study and the earlier results might stem from the double-deficient status of our mice, which lacked both MyD88 and Trif. Therefore, BM chimeric mice were generated in which donors and/or recipients were either WT (CD45.1) or Trif-deficient. No differences could be detected between any of the chimeric mice tested, indicating no significant role for Trif signaling in the setting of DSS colitis (Fig. 1C).

EGFR Ligands AREG and EREG Are Induced by LPS and the Microbiota.

To understand the mechanism behind TLR-mediated protection in experimental colitis, array analysis was performed using the Affymetrix MoGene-1-st-v1 chip, comparing RNA from wild-type colon epithelial cells with RNA from MyD88/Trif double-deficient epithelial cells. The Limma method identified 250 differentially expressed genes that showed significant differential expression by the False Discovery Rate < 0.10. The heatmap in Fig. 2A shows the mean-scaled expression for these transcripts. Two differently regulated genes were the EGFR ligands AREG and EREG. To confirm this observation, real-time analysis for *Areg* and *Ereg* transcripts was performed with epithelial RNA from the colons of wild-type mice and MyD88/Trif double-deficient mice. *Areg* and *Ereg* transcripts were both significantly reduced in MyD88/Trif double-deficient epithelial cells as compared with WT epithelial cells (Fig. 2B). Interestingly, not all EGFR ligand transcripts were dependent on MyD88/Trif signaling. Only *Areg* and *Ereg* transcripts reached statistical significance. No statistically significant difference was found in the levels of *Hbegf*, *Btc*, *Egf*, and *Tgfa* transcripts when MyD88/Trif double-deficient cells and wild-type cells were compared (Fig. 2B).

To determine whether diminished levels of EGFR ligand expression might be responsible for the colitis phenotype observed in MyD88/Trif double-deficient mice, recombinant AREG was injected daily into these animals. Injection of AREG into MyD88/Trif double-deficient mice caused significantly less weight loss compared with that observed in PBS-injected control animals (Fig. 2C).

Next we determined whether TLR ligands are able to induce EGF ligands in the colon of wild-type mice in vivo. Fig. 2D demonstrates that both *Areg* and *Ereg* transcripts are induced in colonic epithelial cells upon systemic LPS challenge. In contrast, no statistically significant induction was found for *Hbegf*, *Egf*, *Tgf*, and *Btc* (Fig. 2D). We considered that the commensal flora might serve as a tonic stimulus for the induction of EGFR ligands AREG and EREG in the intestinal tract. To examine this possibility, the expression of EGFR ligands was measured after the depletion of the flora with antibiotics using vancomycin, neomycin, and metronidazole, administered for 7 d as described previously (22). Administration of broad-spectrum antibiotics significantly diminished the levels of *Areg* and *Ereg* but not of *Hbegf*, *Tgf*, and *Btc* transcripts. *Egf* expression was also significantly reduced, although no differences were observed after LPS stimulation (Fig. 2E). These results indicate that the microbial
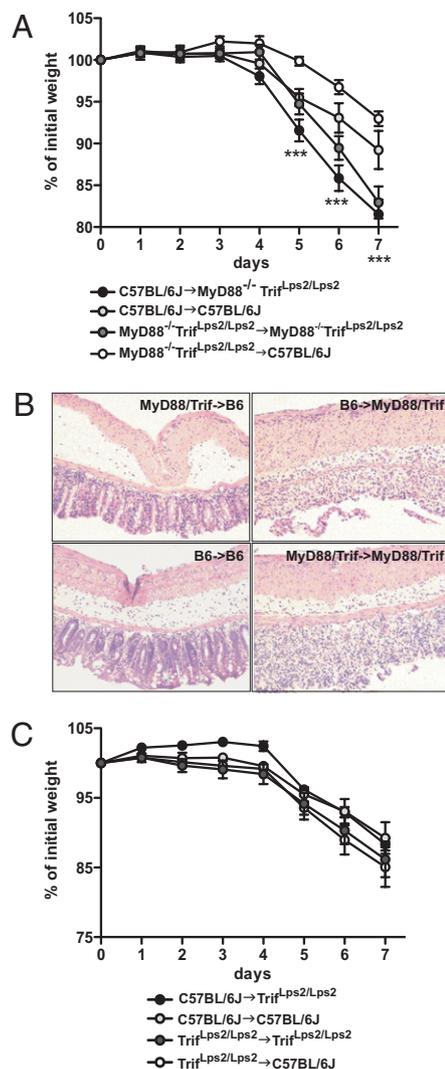

Fig. 1. MyD88 signals in nonhematopoietic cells facilitate susceptibility to acute DSS colitis. (A) Bone marrow chimeras were generated and percent initial weight was determined for 7 d after 2% DSS administration (n = 5 for $Myd88^{-/-}/Trif^{Lps2/Lps2}→Myd88^{-/-}/Trif^{Lps2/Lps2}$ and n = 8–10 for all other groups; ***$P ≤ 0.001$ for $Myd88^{-/-}/Trif^{Lps2/Lps2}→C57BL/6J$ versus C57BL/6J→$Myd88^{-/-}/Trif^{Lps2/Lps2}$, Mann–Whitney test). (B) Representative photomicrographs (magnification 200×; H&E staining) of colons from different chimeric mice 7 d after 2% DSS administration. (C) Percentage of initial weight from different $Trif^{Lps2/Lps2}$ BM chimeras after 2% DSS administration for 7 d (n = 3 for $Trif^{Lps2/Lps2}→Trif^{Lps2/Lps2}$ and n = 5 for all other groups).
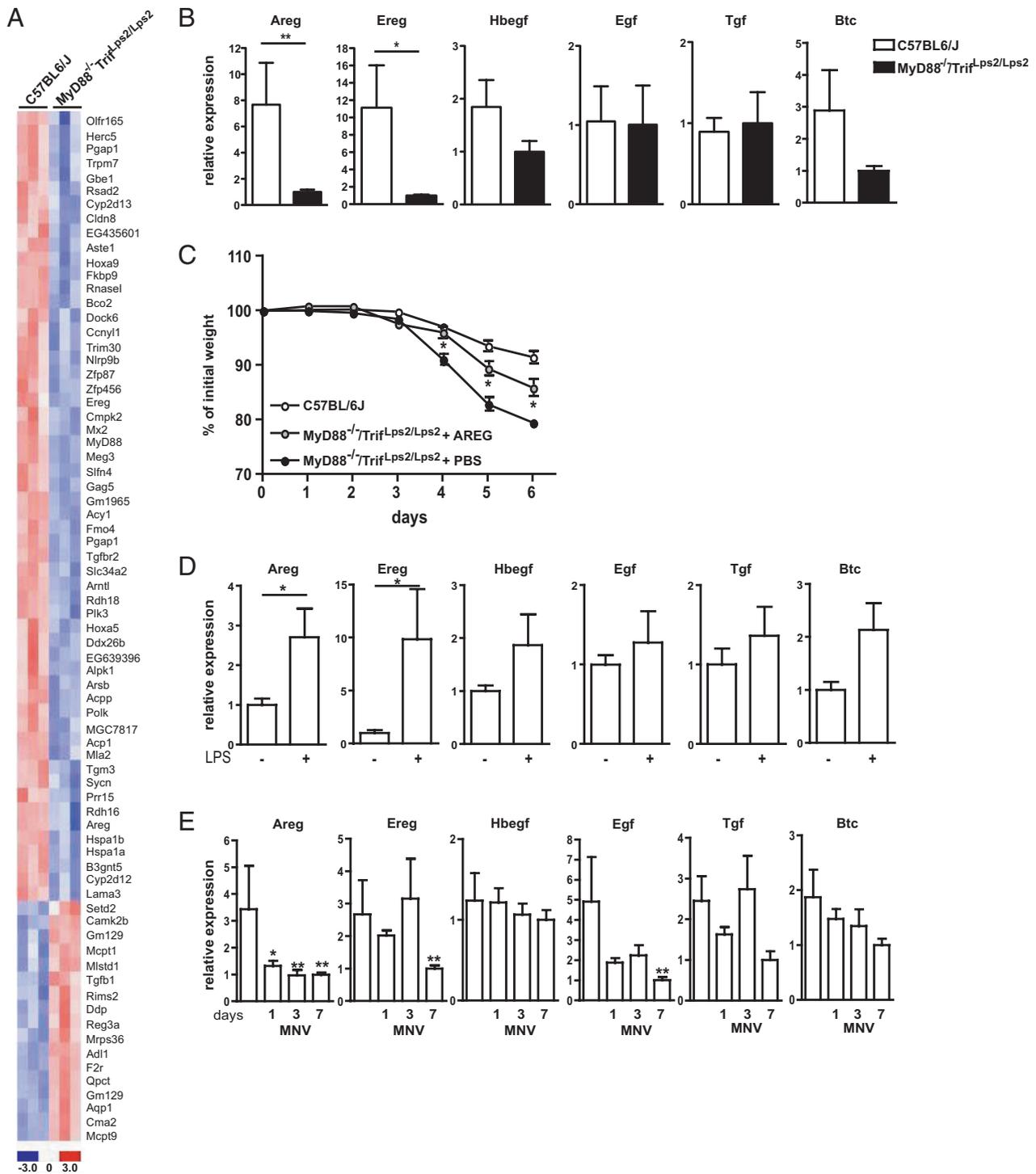
Fig. 2. TLR-mediated signals are important for Areg and Ereg induction. (*A*) Gene expression analysis of epithelial cells from C57BL/6J and *Myd88*^{−/−}/*Trif*[Lps2/Lps2] double-deficient mice. The heatmap shows the mean-scaled expression for differently regulated transcripts. (*B*) mRNA from epithelial cells of *Myd88*^{−/−}/*Trif*[Lps2/Lps2] double-deficient mice were analyzed for the expression of different EGFR ligands. Expression levels were normalized to β-actin. Values shown are expressed relative to the expression of *Myd88*^{−/−}/*Trif*[Lps2/Lps2] double-deficient epithelial cells (*n* = 5–6; *$P \le 0.05$, **$P \le 0.01$, Mann–Whitney test). (*C*) Percentage of initial weight from C57BL/6J and *Myd88*^{−/−}/*Trif*[Lps2/Lps2] double-deficient mice treated with either AREG or PBS daily. All mice received 2% DSS in drinking water for 6 d. *P* values were calculated for *Myd88*^{−/−}/*Trif*[Lps2/Lps2] double-deficient mice treated with AREG versus PBS (*n* = 4–5; *$P \le 0.05$, Mann–Whitney test). (*D*) mRNA expression of different EGFR ligands in C57BL/6J epithelial cells before or 2 h after LPS administration (i.p.). Expression levels were normalized to β-actin or 18s. Values shown are expressed relative to the expression in C57BL/6J epithelial cells before LPS administration (*n* = 5–6; *$P \le 0.05$, Mann–Whitney test). (*E*) mRNA was extracted from the colon of wild-type mice and mice receiving antibiotics (MNV) for 1, 3, and 7 d. Different EGFR ligand expression was examined by quantitative real-time PCR. Expression levels were normalized to β-actin. Values shown are expressed relative to the expression of wild-type mice receiving no treatment (*n* = 6–14 mice per group; *$P \le 0.05$, **$P \le 0.01$, each compared with untreated, Mann–Whitney test).

Brandl et al.

flora is important for the tonic expression of RNA encoding the EGFR ligands AREG, EREG, and EGF.

Mice with Mutations in the EGFR Signaling Pathway Are More Susceptible to DSS-Induced Colitis. We designed a screen to recover mutants with exaggerated susceptibility to DSS, carried out by administering a subpathologic concentration of DSS (1% in drinking water) to ENU-mutagenized mice. Wild-type mice do not show significant weight loss upon administration of 1% DSS in drinking water. However, we found several mice with ENU-induced mutations that showed significant weight loss with 1%

DSS in drinking water for 7 d. Two of these sensitizing mutations were implicated in EGFR signaling. *Velvet* (12), a dominant mutation of *Egfr*, caused significant weight loss in the heterozygous state as compared with wild-type mice when 2% DSS was administered in drinking water (Fig. 3A). *WavedX*, initially noted because of its wavy coat, also scored positive in the sensitized screen. When mapped and positionally cloned (Fig. S1A), *wavedX* was found to correspond to a T→A transversion at position 1186 in exon 9 (of 19 total exons) of *Adam17*, altering a phenylalanine to an isoleucine in the metalloprotease domain of the encoded protein (Fig. 3B). The severe underrepresen-
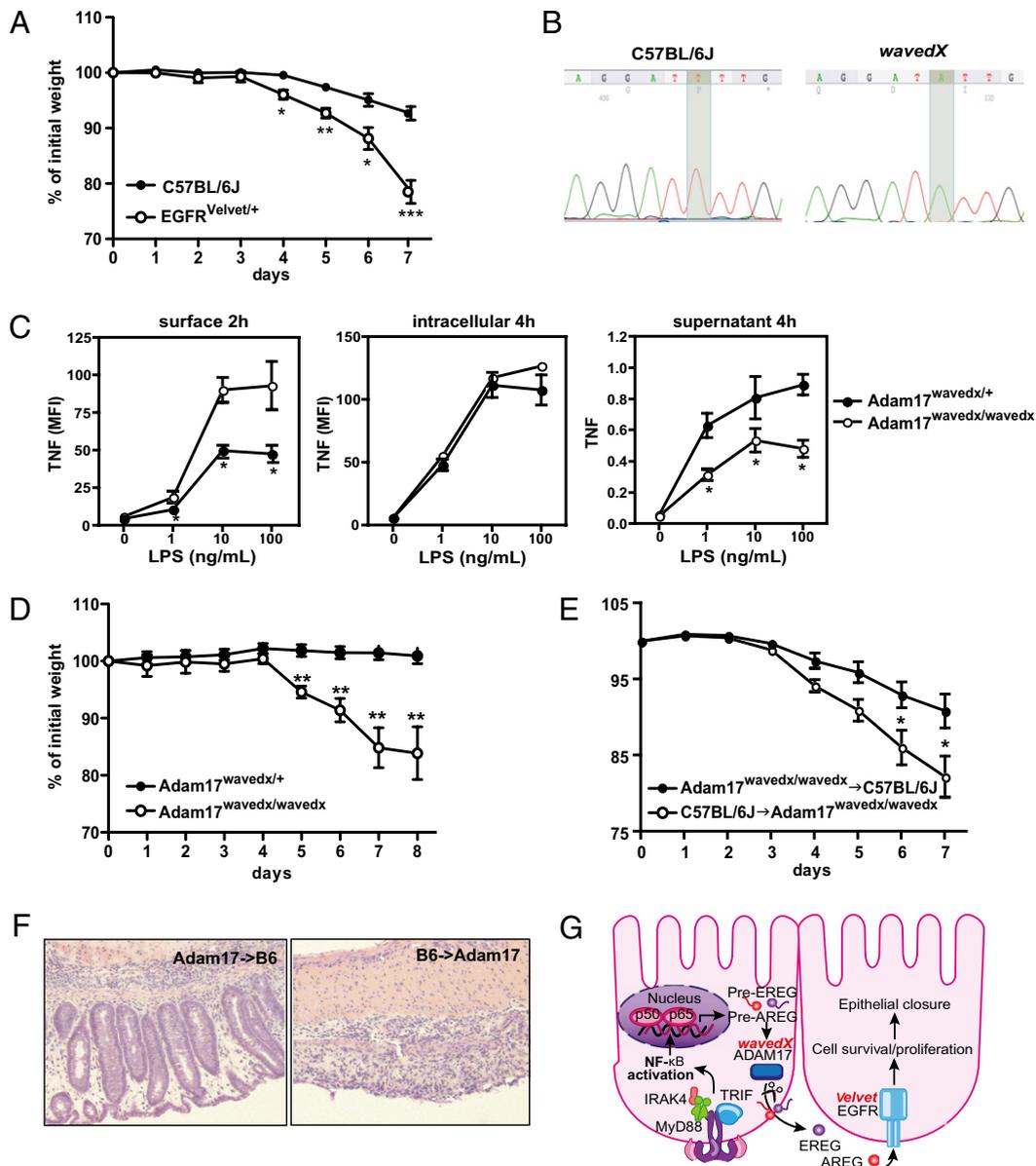

Fig. 3. Mice with defects in EGFR signaling are highly susceptible to DSS-induced colitis. (*A*) Body weight of C57BL/6J and *Egfr*$^{+/Velvet}$ mice after the onset of treatment with DSS. *$P \leq 0.05$, **$P \leq 0.01$, ***$P \leq 0.001$, Mann-Whitney test, $n = 6$–10. (*B*) The *wavedX* mutation corresponds to a T→A transversion at position 1186 of the *Adam17* transcript. (*C*) Macrophages were stimulated with LPS, and surface (*Left*) or intracellular (*Middle*) TNF was measured by flow cytometry. TNF in the supernatant (*Right*) was determined by ELISA after 4-h incubation with different LPS concentrations (*$P \leq 0.05$, Mann–Whitney test, $n = 4$ for Adam17$^{+/wavedX}$ and $n = 5$ for Adam17$^{wavedX/wavedX}$). Error bars denote SD. MFI, mean fluorescence intensity. (*D*) Percent initial weight of Adam17$^{+/wavedX}$ mice and Adam17$^{wavedX/wavedX}$ mice ($n = 10$ for Adam17$^{+/wavedX}$ and $n = 4$ for Adam17$^{wavedX/wavedX}$) after 2% DSS administration. **$P \leq 0.01$, Mann-Whitney test. (*E*) Adam17$^{wavedX/wavedX}$ BM chimeras were generated and percent of initial weight was determined after the onset of treatment with DSS for 8 d ($n = 9$–12 each group; *$P \leq 0.05$, Mann–Whitney test). (*F*) Representative photomicrographs (magnification 200×; H&E staining) of colons from different chimeric mice 7 d after 2% DSS administration. (*G*) Model of a TLR→MyD88→EGFR ligand→EGFR signaling pathway in nonhematopoietic cells of the intestinal tract.

tation of *Adam17* knockout mice at weaning age (23) was not observed in *wavedX* homozygotes, whose survival rate (16.07%) was only slightly lower than the expected Mendelian ratio of 25% (Fig. S1*B*) (23). SDS/PAGE analysis indicated that predominantly unprocessed ADAM17 was present in primary embryonic fibroblasts from *Adam17*$^{wavedX/wavedX}$ mice (Fig. S2*A*), and sheddase activity of the mutant was impaired. LPS-stimulated peritoneal macrophages from *wavedX* homozygotes showed increased surface expression of TNF and secreted diminished quantities of mature, soluble TNF, whereas intracellular TNF levels were not affected (Fig. 3*C*). Proteolytic cleavage of ADAM17 substrates can occur in response to phorbol 12-myristate 13-acetate (PMA) or LPS. Shedding of two other ADAM17 substrates, L-selectin (induced by PMA) and FLT3L (induced by LPS), were also both impaired in *wavedX* homozygotes (Fig. S2 *B* and *C*). When embryonic fibroblasts from *wavedX* homozygotes or heterozygotes were stimulated with PMA, *wavedX/wavedX* cells secreted less alkaline phosphatase (AP)-tagged TNF and TGF-α than the controls (Fig. S2*D*).

WavedX/wavedX mice showed severe weight loss compared with wild-type mice during DSS administration (Fig. 3*D*). To evaluate the importance of ADAM17 in epithelial cells versus hematopoietic cells, bone marrow chimeric mice were generated in which donors and/or recipients were either wild-type (CD45.1) or *Adam17*$^{wavedX/wavedX}$ mutants (CD45.2). Chimerized *Adam17*$^{wavedX/wavedX}$ mice with wild-type hematopoietic cells showed significant weight loss compared with chimeric mice with *Adam17*$^{wavedX/wavedX}$ hematopoietic cells (Fig. 3*E*). Histologic examination of different chimeric mice revealed dramatic leukocyte infiltration and a complete loss of epithelial architecture in chimerized *Adam17*$^{wavedX/wavedX}$ mice. In contrast, wild-type mice receiving *Adam17*$^{wavedX/wavedX}$ bone marrow only showed mild leukocyte infiltration. The epithelial architecture in these mice was relatively undisturbed (Fig. 3*F*).

Discussion

Here we have presented evidence that TLR signaling operates in radioresistant cells of the gastrointestinal tract, where it induces EGF ligands AREG and EREG, triggering a protective response in radioresistant cells via EGFR. TLRs are expressed in many different cells of the intestinal tract: in the hematopoietic compartment on dendritic cells, macrophages, and lymphocytes, and within the nonhematopoietic compartment of the epithelial cell monolayer on both the basolateral and apical surfaces of these cells (24). Although several studies have shown an important role for TLR signaling in different models of acute and chronic intestinal inflammation, it is less clear which cells mediate different phenotypes.

Several recent studies have shown a protective role for TLR signaling in acute models of intestinal inflammation. MyD88-deficient mice are more susceptible to several intestinal bacteria and pathogens such as *Listeria monocytogenes* (25), vancomycin-resistant *Enterococcus* (22), *Salmonella typhimurium* (26, 27), and *Citrobacter rodentium* (28). Also, it has been shown by several groups that MyD88 signaling is protective in a model of acute induced colitis (5, 6, 29).

In the setting of an acute infectious intestinal inflammation, we have shown previously for *L. monocytogenes* and vancomycin-resistant *Enterococcus faecium* that MyD88 signaling plays an important role in nonhematopoietic cells by inducing the antimicrobial molecule RegIIIγ, which is important for defense against Gram-positive bacteria (22, 25). In line with these results, we find now that TLR signaling in nonhematopoietic cells is crucial in a model of DSS-induced colitis. Within the nonhematopoietic compartment, it is most likely that epithelial cells are responsible for the phenotype. However, we cannot exclude a role of radioresistant hematopoietic cells. Studies with cell-specific deletions will be necessary to ascertain the exact cell type.

Our findings contrast with data previously published by Rakoff-Nahoum et al. showing that hematopoietic cells, presumably macrophages, confer the DSS colitis phenotype (11). Although these authors used MyD88-deficient mice, in contrast to the MyD88/Trif double-deficient mice used in our study, we have shown that the adaptor molecule Trif makes no contribution to protection against DSS-induced colitis (Fig. 1*C*) and are unable to account for the discrepancy on this basis.

Whereas TLR signaling is protective in acute intestinal inflammation, it seems to be detrimental in chronic intestinal inflammation. Using a model of *Helicobacter hepaticus*-induced chronic inflammation, a recent study showed MyD88 signaling in leukocytes to be responsible for the phenotype (30). Also, using IL-10-deficient mice as a model of chronic T cell-dependent colitis, depletion of IKKβ in the myeloid compartment prolongs survival. In contrast, mice selectively deficient for IKKβ in intestinal epithelial cells showed a severe phenotype in the acute DSS colitis model (31). Taken together, these results suggest that MyD88 signaling in nonhematopoietic cells plays an important role in acute intestinal inflammation, whereas MyD88 signaling in myeloid cells mediates susceptibility in chronic inflammation.

MyD88/Trif double-deficient epithelial cells showed decreased levels of the EGFR ligands AREG and EREG, both of which could be induced by systemic LPS administration. Other studies have previously also linked TLR signaling with EGFR activation (18, 20, 21, 32), and EGFR phosphorylation was reduced in the colons of TLR4-deficient mice (32). However, our studies show in vivo induction of EGFR ligands upon LPS administration, which implies a coaxial pathway linking TLR signaling with EGFR-signaling.

EGFR activation aids in growth, repair, and barrier integrity in the gastrointestinal tract. Several studies have shown an important role for EGFR signaling in mouse models of induced colitis. Mice with mutations affecting EGFR signaling, including *Egfr*$^{waved2/waved2}$, *Tgfa*$^{-/-}$, *Tgfa*$^{waved1/waved1}$, and *Ereg*$^{-/-}$ mice, show increased susceptibility to DSS-induced colitis (14, 17, 33). Also, reconstitution experiments show that different EGFR ligands improve colitis (13, 17, 33). In the present study, we report that EGFR signaling is specifically of importance in nonhematopoietic cells. Furthermore, we find that only the EGFR ligands AREG and EREG are regulated by TLR signaling. However, we cannot exclude complete TLR independency of other EGFR ligands, as EGF was also significantly down-regulated in mice treated 7 d with broad-spectrum antibiotics. Others have reported different kinetics in the induction of *Areg* and *Ereg*. Whereas *Ereg* was predominantly up-regulated during acute mucosal injury, *Areg* expression was seen specifically during chronic inflammation. TLR4-deficient mice did not show any significant induction of *Areg* and *Ereg* (21). Based on reconstitution studies with MyD88/Trif double-deficient mice, our data provide evidence that AREG plays an important role in an acute model of colitis.

In conclusion, a TLR→MyD88→[AREG/EREG]→EGFR signaling pathway exists in nonhematopoietic cells of the intestinal tract, where it acts to sense and respond to microbial invasion. This pathway depends upon the processing role of ADAM17 and mediates protection against DSS-induced colitis (Fig. 3*G*).

Materials and Methods

ENU Mutagenesis. C57BL/6J and C57BL/6J Ly5.1 congenics were purchased from The Jackson Laboratory. All mice were kept and bred in The Scripps Research Institute vivarium under the supervision of the Department of Animal Resources. All animal procedures were approved by the Institutional Animal Care and Use Committee and performed according to institutional guidelines for animal care. C57BL/6J mice were used for ENU mutagenesis to generate the *Velvet* and *wavedX* strains, as described (http://mutagenetix.scripps.edu).

IMMUNOLOGY

Mapping and Sequencing. *WavedX* males were mated to C3H/HeN females and the offspring intercrossed. The progeny of the F2 generation was phenotyped and genotyped for mapping by analyzing 127 microsatellite markers for genome-wide linkage analysis (Fig. S1A). The *Velvet* mutation was mapped and identified as described previously (12).

Induction of DSS Colitis, and LPS and AREG Administration. Sex- and age-matched littermates received 2% DSS (MP Biomedicals) in drinking water for 6–7 d. Weight was recorded daily. Gut commensal depletion was performed as described previously (34). In some experiments, mice were given daily doses (10 μg per mouse) of recombinant AREG (Leinco Technologies) or PBS by i.p. injection. For induction of EGFR ligands, mice were i.p. injected with 200 μg LPS (from *S. typhimurium*; Alexis Biochemicals). Epithelial cells were isolated 2 h after LPS injections.

Histology. Freshly isolated colon was fixed in formalin and embedded in paraffin. H&E staining was performed using a standard protocol.

Real-Time PCR Analysis. Colonic RNA was isolated using the TRIzol reagent (Invitrogen). DNase-treated RNA was used in randomly primed cDNA synthesis and real-time PCR analysis. SYBR green-based real-time PCR was performed using the DyNAmo SYBR Green qPCR Kit (Finnzymes). Primers were designed using National Institutes of Health qPrimerdepot software. Signals were normalized to β-actin or 18s. Normalized data were used to measure relative expression levels of different genes using $\Delta\Delta Ct$ analysis.

Generation of BM Chimeric Mice. Generation of BM chimeric mice was performed as recently described (34). Recipient WT (CD45.1) or $Myd88^{-/-}$; $Trif^{Lps2/Lps2}$ or $Adam17^{wavedX/wavedX}$ (CD45.2) mice were lethally irradiated with 950 rad using a ^{137}Cs source and injected i.v. 2–3 h later with 5×10^6 BM cells derived from the tibia and femurs of the respective donors. Seven weeks after engrafting, reconstitution was assessed by FACS analysis of blood leukocytes.

Epithelial Cell Isolation. Colonic epithelial cells of WT and $Myd88^{-/-}$/$Trif^{Lps2/Lps2}$ double-deficient mice were isolated as described previously (34).

Microarray Analysis. RNA was extracted from epithelial cells with TRIzol (Invitrogen) and purified with Qiagen RNeasy according to the manufacturer's instructions. RNA quality was analyzed with an Agilent Bioanalyzer. Samples were hybridized to an Affymetrix Mouse Gene 1.0 ST Array using standard Affymetrix protocols. The raw expression values were normalized by using robust multichip average (RMA) (35). Differential expression was determined using the Limma package (36) in R software. The adjusted *P* value is the *P* value adjusted for multiple testing using Benjamini and Hochberg's method to control the false discovery rate (35). Heatmaps and clustering were generated with the dChip program (www.dChip.org). Red indicates increased expression and blue indicates decreased expression relative to the mean transcript expression.

Detection of TNFα, L-Selectin, and FLT3L. Intracellular, secreted, and surface-expressed TNFα were measured as previously described (37). For the measurement of L-selectin shedding, 1×10^6 thymocytes were stimulated with the indicated dose of PMA for 30 min, after which surface expression of L-selectin was measured by FACS. For the induction of FLT3L, mice were injected with 50 μg LPS [*Salmonella minnesota* R595 (Re); Enzo Life Sciences], and serum was collected 2 h later. Serum FLT3L was measured by ELISA according to the manufacturer's instructions (R&D Systems).

Statistical Analysis. Statistical analysis was performed using Prism 4.0 software, applying the Mann–Whitney test for unpaired data. All *P* values ≤0.05 were considered significant. $*P \leq 0.05$; $**P \leq 0.01$; $***P \leq 0.001$. Error bars denote SEM unless otherwise indicated.

1. Podolsky DK (2002) Inflammatory bowel disease. *N Engl J Med* 347:417–429.
2. Xavier RJ, Podolsky DK (2007) Unravelling the pathogenesis of inflammatory bowel disease. *Nature* 448:427–434.
3. Yamamoto-Furusho JK, Podolsky DK (2007) Innate immunity in inflammatory bowel disease. *World J Gastroenterol* 13:5577–5580.
4. Sartor RB (2006) Mechanisms of disease: Pathogenesis of Crohn's disease and ulcerative colitis. *Nat Clin Pract Gastroenterol Hepatol* 3:390–407.
5. Rakoff-Nahoum S, Paglino J, Eslami-Varzaneh F, Edberg S, Medzhitov R (2004) Recognition of commensal microflora by Toll-like receptors is required for intestinal homeostasis. *Cell* 118:229–241.
6. Fukata M, et al. (2005) Toll-like receptor-4 is required for intestinal response to epithelial injury and limiting bacterial translocation in a murine model of acute colitis. *Am J Physiol Gastrointest Liver Physiol* 288:G1055–G1065.
7. Brown SL, et al. (2007) Myd88-dependent positioning of Ptgs2-expressing stromal cells maintains colonic epithelial proliferation during injury. *J Clin Invest* 117:258–269.
8. Iqbal N, et al. (2002) T helper 1 and T helper 2 cells are pathogenic in an antigen-specific model of colitis. *J Exp Med* 195:71–84.
9. Nenci A, et al. (2007) Epithelial NEMO links innate immunity to chronic intestinal inflammation. *Nature* 446:557–561.
10. Hugot JP, Zouali H, Lesage S (2003) Lessons to be learned from the NOD2 gene in Crohn's disease. *Eur J Gastroenterol Hepatol* 15:593–597.
11. Rakoff-Nahoum S, Hao L, Medzhitov R (2006) Role of Toll-like receptors in spontaneous commensal-dependent colitis. *Immunity* 25:319–329.
12. Du X, et al. (2004) Velvet, a dominant Egfr mutation that causes wavy hair and defective eyelid development in mice. *Genetics* 166:331–340.
13. Chalaris A, et al. (2010) Critical role of the disintegrin metalloprotease ADAM17 for intestinal inflammation and regeneration in mice. *J Exp Med* 207:1617–1624.
14. Lee D, et al. (2004) Epiregulin is not essential for development of intestinal tumors but is required for protection from intestinal damage. *Mol Cell Biol* 24:8907–8916.
15. Luetteke NC, et al. (1999) Targeted inactivation of the EGF and amphiregulin genes reveals distinct roles for EGF receptor ligands in mouse mammary gland development. *Development* 126:2739–2750.
16. Troyer KL, et al. (2001) Growth retardation, duodenal lesions, and aberrant ileum architecture in triple null mice lacking EGF, amphiregulin, and TGF-α. *Gastroenterology* 121:68–78.
17. Egger B, Büchler MW, Lakshmanan J, Moore P, Eysselein VE (2000) Mice harboring a defective epidermal growth factor receptor (waved-2) have an increased susceptibility to acute dextran sulfate-induced colitis. *Scand J Gastroenterol* 35:1181–1187.
18. Fukata M, et al. (2007) Toll-like receptor-4 promotes the development of colitis-associated colorectal tumors. *Gastroenterology* 133:1869–1881.
19. Koff JL, Shao MX, Ueki IF, Nadel JA (2008) Multiple TLRs activate EGFR via a signaling cascade to produce innate immune responses in airway epithelium. *Am J Physiol Lung Cell Mol Physiol* 294:L1068–L1075.
20. Hernandez Y, et al. (2010) The role of prostaglandin E2 (PGE 2) in Toll-like receptor 4 (TLR4)-mediated colitis-associated neoplasia. *BMC Gastroenterol* 10:82.
21. Hsu D, et al. (2010) Toll-like receptor 4 differentially regulates epidermal growth factor-related growth factors in response to intestinal mucosal injury. *Lab Invest* 90:1295–1305.
22. Brandl K, et al. (2008) Vancomycin-resistant enterococci exploit antibiotic-induced innate immune deficits. *Nature* 455:804–807.
23. Peschon JJ, et al. (1998) An essential role for ectodomain shedding in mammalian development. *Science* 282:1281–1284.
24. Abreu MT (2010) Toll-like receptor signalling in the intestinal epithelium: How bacterial recognition shapes intestinal function. *Nat Rev Immunol* 10:131–144.
25. Brandl K, Plitas G, Schnabl B, DeMatteo RP, Pamer EG (2007) MyD88-mediated signals induce the bactericidal lectin RegIIIγ and protect mice against intestinal *Listeria monocytogenes* infection. *J Exp Med* 204:1891–1900.
26. Hapfelmeier S, et al. (2008) Microbe sampling by mucosal dendritic cells is a discrete, MyD88-independent step in ΔinvG *S. typhimurium* colitis. *J Exp Med* 205:437–450.
27. Hapfelmeier S, et al. (2005) The Salmonella pathogenicity island (SPI)-2 and SPI-1 type III secretion systems allow *Salmonella* Serovar *typhimurium* to trigger colitis via MyD88-dependent and MyD88-independent mechanisms. *J Immunol* 174:1675–1685.
28. Gibson DL, et al. (2008) MyD88 signalling plays a critical role in host defence by controlling pathogen burden and promoting epithelial cell homeostasis during *Citrobacter rodentium*-induced colitis. *Cell Microbiol* 10:618–631.
29. Araki A, et al. (2005) MyD88-deficient mice develop severe intestinal inflammation in dextran sodium sulfate colitis. *J Gastroenterol* 40:16–23.
30. Asquith MJ, Boulard O, Powrie F, Maloy KJ (2010) Pathogenic and protective roles of MyD88 in leukocytes and epithelial cells in mouse models of inflammatory bowel disease. *Gastroenterology* 139:519–529.e2.
31. Eckmann L, et al. (2008) Opposing functions of IKKβ during acute and chronic intestinal inflammation. *Proc Natl Acad Sci USA* 105:15058–15063.
32. Fukata M, et al. (2006) Cox-2 is regulated by Toll-like receptor-4 (TLR4) signaling: Role in proliferation and apoptosis in the intestine. *Gastroenterology* 131:862–877.
33. Egger B, et al. (1997) Mice lacking transforming growth factor α have an increased susceptibility to dextran sulfate-induced colitis. *Gastroenterology* 113:825–832.
34. Brandl K, et al. (2009) Enhanced sensitivity to DSS colitis caused by a hypomorphic Mbtps1 mutation disrupting the ATF6-driven unfolded protein response. *Proc Natl Acad Sci USA* 106:3300–3305.
35. Benjamini Y, Hochberg Y (1995) Controlling the false discovery rate: A practical and powerful approach to multiple testing. *J R Stat Soc Series B Stat Methodol* 57:289–300.
36. Smyth GK (2004) Linear models and empirical Bayes methods for assessing differential expression in microarray experiments. *Stat Appl Genet Mol Biol*, 3: Article 3.
37. Siggs OM, et al. (2010) A mutation of Ikbkg causes immune deficiency without impairing degradation of IκBα. *Proc Natl Acad Sci USA* 107:3046–3051.